Motion of CO Molecules in Solid C$_{60}$ Probed by Solid-State NMR

Iwan Holleman,[*,†] **Pierre Robyr,**[‡] **Arno P. M. Kentgens,**[†] **Beat H. Meier,**[†,‡] **and Gerard Meijer**[†]

Contribution from the NSR Center and Research Institute for Materials, University of Nijmegen, Toernooiveld, NL-6525 ED Nijmegen, The Netherlands, and Laboratory for Physical Chemistry, ETH Zentrum, CH-8092 Zürich, Switzerland

Received July 15, 1998. Revised Manuscript Received October 30, 1998

Abstract: Polycrystalline C$_{60}$ has been intercalated with 99 atom % ^{13}C-enriched CO gas by using high-pressure, high-temperature synthesis. The ratio of ^{13}CO to C$_{60}$ is determined using ^{13}C NMR under magic-angle spinning and is found to be almost 1:2. Static solid-state ^{13}C NMR spectra of ^{13}CO-intercalated C$_{60}$ have been measured in the range between room temperature and 4 K. In the high-temperature range, i.e., between room temperature and 100 K, the CO molecules in the "octahedral" sites of the C$_{60}$ lattice reorient rapidly on the NMR time scale. At 4 K the reorientation rate of CO is so low that, on the NMR time scale, the molecule appears localized in one of the minima of the potential. Between 4 and 30 K, the transition from the static to the dynamic regime can be inferred from NMR line shape changes. The temperature dependence of the line shape is modeled in terms of thermally activated jump-like reorientations of the CO molecules in the C$_{60}$ lattice. No evidence for a quantum mechanical coherent tunneling motion of the CO molecules in the octahedral sites of the C$_{60}$ lattice has been found.

Introduction

Recently, we have reported that CO gas can be intercalated into the octahedral sites of the C$_{60}$ lattice using high-pressure, high-temperature synthesis.[1] A large fraction of the octahedral sites can be occupied, and a ratio of CO to C$_{60}$ up to 1:1 can in principle be reached in the solid. Under ambient conditions CO-intercalated C$_{60}$ is a stable compound. The motion of the CO molecule in the octahedral site has been studied as a function of temperature by infrared (IR) and nuclear magnetic resonance (NMR) spectroscopy, and the results have been compared to quantum mechanical calculations. The observed spectra indicate a nearly free rotational motion of CO at room temperature, with a gradual transition to hindered rotational motion of CO at low temperature.[1] From the agreement between the measured and the calculated IR spectra of CO-intercalated C$_{60}$ as a function of the size of the octahedral site, it has been concluded that CO-intercalated C$_{60}$ truly behaves as a "molecule in a box".[2] The simplicity of the NMR spectrum of CO-intercalated C$_{60}$, due to the presence of only two resonances and the small dipolar coupling in the sample, allows the study of the dynamics of CO intercalated in C$_{60}$ by solid-state ^{13}C NMR in a rather straightforward manner.

NMR measurements have played an important role in the elucidation of the structural and dynamical properties of both dissolved and crystalline C$_{60}$. In 1990, the proposed truncated icosahedral (I_h) structure for C$_{60}$, in which all 60 carbon atoms are symmetry equivalent, has been confirmed by the observation of a single ^{13}C NMR line for C$_{60}$.[3,4] The static solid-state ^{13}C NMR spectra of crystalline C$_{60}$ showed a rapid isotropic rotational motion of C$_{60}$ in the solid at room temperature,[5] which clarified the nature of the orientational disorder that had hampered further analysis of room-temperature X-ray diffraction data. The orientational ordering phase transition in crystalline C$_{60}$[6] has been observed by solid-state ^{13}C NMR via a discontinuity in the T_1 relaxation time of C$_{60}$.[7] Using the dependence of T_1 on the orientational correlation time, Johnson *et al.* characterized the high-temperature (rotator) and low-temperature (ratchet) phases of crystalline C$_{60}$ and determined the Arrhenius activation energies and preexponential factors of both phases.[8] Furthermore, the length of the 60 pentagon bonds and that of the 30 interpentagon bonds in the C$_{60}$ molecule have been determined for the first time in a solid-state NMR measurement as 1.45 and 1.40 Å, respectively, from the ^{13}C–^{13}C dipolar coupling in partially ^{13}C-enriched C$_{60}$ using the Carr–Purcell sequence.[9]

Various derivatives of C$_{60}$ have been investigated by NMR spectroscopy as well. Saunders *et al.* have probed the interior of fullerenes by ^{3}He NMR spectroscopy of endohedral (inside the cage) ^{3}He@C$_{60}$ and ^{3}He@C$_{70}$ and have found unexpectedly large shieldings, indicating significant diamagnetic ring currents in C$_{60}$ and very large ones in C$_{70}$.[10] Details on the electronic properties of the superconducting alkali metal intercalated C$_{60}$

---

(1) Holleman, I.; von Helden, G.; Olthof, E. H. T.; van Bentum, P. J. M.; Engeln, R.; Nachtegaal, G. H.; Kentgens, A. P. M.; Meier, B. H.; van der Avoird, A.; Meijer, G. *Phys. Rev. Lett.* **1997**, *79*, 1138–1141.

(2) Holleman, I.; von Helden, G.; van der Avoird, A.; Meijer, G. *Phys. Rev. Lett.* **1998** *80*, 4899–4902.

(3) Taylor, R.; Hare, J. P.; Abdul-Sada, A. K.; Kroto, H. W. *J. Chem. Soc., Chem. Commun.* **1990**, *20*, 1423–1425.

(4) Johnson, R. D.; Meijer, G.; Bethune, D. S. *J. Am. Chem. Soc.* **1990**, *112*, 8983–8984.

(5) Yannoni, C. S.; Johnson, R. D.; Meijer, G.; Bethune, D. S.; Salem, J. R. *J. Phys. Chem.* **1991**, *95*, 9–10.

(6) Heiney, P. A.; Fischer, J. E.; McGhie, A. R.; Romanow, W. J.; Denenstein, A. M.; McCauley, J. P., Jr.; Smith, A. B., III; Cox, D. E. *Phys. Rev. Lett.* **1991**, *66*, 2911–2914. Sachidanandam, R.; Harris, A. B. *Phys. Rev. Lett.* **1991**, *67*, 1467–1468.

(7) Tycko, R.; Dabbagh, G.; Fleming, R. M.; Haddon, R. C.; Makhija, A. V.; Zahurak, S. M. *Phys. Rev. Lett.* **1991**, *67*, 1886–1889.

(8) Johnson, R. D.; Yannoni, C. S.; Dorn, H. C.; Salem, J. R.; Bethune, D. S. *Science* **1992**, *255*, 1235–1238.

(9) Yannoni, C. S.; Bernier, P. P.; Bethune, D. S.; Meijer, G.; Salem, J. R. *J. Am. Chem. Soc.* **1991**, *113*, 3190–3192.

compounds (A_3C_{60}, A = K, Rb, Cs) have been obtained from measurements of T_1 relaxation times and NMR frequency shifts (Knight shifts) as a function of temperature.[11] The presence of molecular oxygen in the octahedral sites of crystalline C_{60} has been evidenced by solid-state ^{13}C NMR via the observed shifting of the C_{60} resonance due to the Fermi-contact interaction between the paramagnetic oxygen molecules and the C_{60} molecules.[12]

Here we report a detailed study on the motion of CO molecules intercalated in crystalline C_{60} as a function of temperature in the region between 295 and 4 K, using solid-state ^{13}C NMR. The measurements indicate that the CO molecules rapidly reorient on the NMR time scale in the region between 295 and 100 K and that they function as sensitive probes of the local symmetry of the C_{60} lattice. At 4 K the reorientation of the CO molecules has stopped on the NMR time scale, and the molecule appears localized in one of the minima of the potential. Between 4 and 30 K the onset of the reorientational motion of the CO molecule is witnessed via changes in the ^{13}C NMR line shape. We use a simplified chemical-exchange model based on the classical McConnell equation[13] to describe the observed solid-state ^{13}C NMR spectra. In this model, a CO molecule can make thermally activated jumps between different orientations in an octahedral site of the C_{60} lattice.

Background Information on CO-Intercalated C_{60}. In this section some relevant details on the structure and the phase transitions of (CO-intercalated) C_{60} will be given. In addition, the interaction potential between a CO molecule and the surrounding C_{60} molecules will be discussed.

It is well-established by now that the structure of crystalline pristine C_{60} at room temperature is face-centered cubic (fcc)[14] and that the C_{60} molecules rotate rapidly and isotropically in the solid.[5] At 260 K, the C_{60} crystal transforms via an orientational ordering phase transition to a simple-cubic (sc) lattice with a crystal symmetry of $Pa\bar{3}$.[6] At this orientational ordering transition, the four C_{60} molecules in the fcc unit cell remain (more or less) at the same position, but the isotropic rotation of the molecules abruptly stops, and they become orientationally inequivalent. The crystal structure in which these four molecules have distinct, but symmetry-related, orientations can be described with four interpenetrating simple-cubic lattices, with the same lattice constant as that of the conventional fcc unit cell. A detailed description of the order and disorder in fullerenes can be found in the review article by Fischer and Heiney.[14] The solid-state NMR line shape of C_{60} remains narrow and symmetric while passing this phase transition, as the C_{60} molecules are still jumping between symmetry-equivalent orientations in the sc phase. This motion interchanges all the corners of the icosahedron and leads to a complete averaging of the chemical shift anisotropy which is a second-rank tensor. A jump in the T_1 relaxation time is the only clue of this phase transition in NMR.[7,8] Apart from rotational jumps between symmetry-equivalent orientations, the C_{60} molecules are also jumping between two symmetry-inequivalent orientations, commonly denoted as the p-orientation and the h-orientation. In a hypothetical crystal with all C_{60} molecules in the p-orientation,

each C_{60} molecule would have six of its electron-poor *p*entagons facing the electron-rich interpentagon bonds of six of its twelve neighbors. In a hypothetical crystal with only h-oriented C_{60} molecules, electron-poor *h*exagons of a C_{60} molecule are facing interpentagon bonds on its neighbors.[15] A pictorial presentation of these two possible orientations is given by Copley *et al*.[16] (Figure 5 of this reference). In a real C_{60} crystal the *p*- and *h*-orientation are thought to be intimately mixed and the probability p (h) of finding a C_{60} molecule in the p-orientation (h-orientation) depends on the temperature. When the temperature is decreased, the energetically preferred p-orientation gains in probability relative to the h-orientation. At the same time the jump rate between the different orientations decreases. Below the glass-transition temperature, the exact value of which depends on the time scale of the experiment, the C_{60} molecules appear fixed in either the p- or h-orientation. In neutron diffraction studies, the glass transition of C_{60} is found around 90 K. For temperatures below this, the ratio of the p-oriented to h-oriented C_{60} molecules remains constant at an approximate value of 5:1.[15] In passing the temperature of the glass transition in an NMR experiment, somewhere between 150 and 100 K, the NMR line shape of C_{60} changes from an isotropic line to a CSA tensor pattern.[5]

In the cubic lattice of C_{60} (both fcc and sc) two types of interstitial sites are available for intercalants, one large octahedral site and two smaller tetrahedral sites per C_{60} molecule. The octahedral site can contain a sphere with a diameter of 4.1 Å and is the only site in which a CO molecule snugly fits.[1] The octahedral site is located at the center of the conventional cell of the fcc lattice. In an fcc lattice of perfect spheres, which is a good approximation for solid C_{60} at room temperature, the symmetry of the octahedral site is O_h. The $Pa\bar{3}$ symmetry of the simple-cubic phase implies that the symmetry of the octahedral site is reduced to S_6 (a C_3 axis and point inversion i are the remaining symmetry elements), if we neglect the disorder between the p- and h-orientation. This neglect is justified above the glass-transition temperature since in this regime the interconversion between both orientations is fast enough that an averaged environment is probed in an NMR experiment. At temperatures below the glass-transition temperature, a further lowering of the site symmetry can occur.

From recent X-ray measurements on CO-intercalated C_{60}, it is concluded that the intercalation with CO does not change the symmetry of the C_{60} crystal and that the CO molecules are located in the octahedral sites indeed. The fcc → sc orientational ordering transition is found at a temperature of 243 K, the possible orientations of C_{60} are the same as found for pristine C_{60}, and below the glass-transition temperature, now at 84 K, the ratio of p- to h-oriented C_{60} molecules remains constant at a value of 12.5:1.[17,18] It should be noted that both the temperature of the phase transitions and the ratio of the p-oriented to the h-oriented molecules depend on the ratio of CO to C_{60} in the sample.

To calculate the potential energy surface for a CO molecule in the octahedral site of the C_{60} lattice, rigid C_{60} molecules (fixed bond lengths) are placed on the lattice in fixed orientations. The interaction of a CO molecule with all of the surrounding C_{60} molecules is calculated as a function of both the orientation

(10) Saunders: M.; Jiménez-Vázquez, H. A.; Cross, R. J.; Mroczkowski, S.; Freedberg, D. I.; Anet, F. A. L. *Nature* **1994**, *367*, 256−257.

(11) Tycko, R.; Dabbagh, G.; Rosseinsky, M. J.; Murphy, D. W.; Ramirez, A. P.; Fleming, R. M. *Phys. Rev. Lett.* **1992**, *68*, 1912−1915.

(12) Assink, R. A.; Schirber, J. E.; Loy, D. A.; Morosin, B.; Carlson, G. A. *J. Mater. Res.* **1992**, *7*, 2136−2143.

(13) McConnell, H. M. *J. Chem. Phys.* **1958**, *28*, 430−431.

(14) Fischer, J. E.; Heiney, P. A. *J. Phys. Chem. Solids* **1993**, *54*, 1725−1757.

(15) David, W. I. F.; Ibberson, R. M.; Dennis, T. J. S.; Hare, J. P.; Prassides, K. *Europhys. Lett.* **1992**, *18*, 219−225 and 735−736.

(16) Copley, J. R. D.; Neumann, D. A.; Cappelletti, R. L.; Kamitakahara, W. A. *J. Phys. Chem. Solids* **1992**, *53*, 1353−1371.

(17) van Smaalen, S.; Dinnebier, R.; Holleman, I.; von Helden, G.; Meijer, G. *Phys. Rev. B* **1998**, *57*, 6321−6324.

(18) van Smaalen, S.; Dinnebier, R.; Schnelle, W.; Holleman, I.; von Helden, G.; Meijer, G. *Europhys. Lett.* **1998**, *43*, 302−307.

of the CO molecule and the position of its center of mass.[1] The resulting potential has eight minima corresponding to a CO molecule oriented parallel or antiparallel to one of the four body diagonals of the conventional cubic cell. With all of the C$_{60}$ molecules in the *h*-orientation the CO molecule is preferentially oriented along the cube diagonal that coincides with the C_3 symmetry axis. In this case, the calculated van der Waals energy difference ΔE_h between the two equivalent minima on the C_3 axis and the six equivalent minima off the C_3 axis is $\Delta E_h = -6$ cm^{-1}. With all of the C$_{60}$ molecules in the *p*-orientation the six minima off the C_3 axis are energetically preferred, and $\Delta E_p = 48$ cm^{-1}. For temperatures between the orientational ordering transition temperature and the glass-transition temperature, all of the C$_{60}$ molecules surrounding the CO molecule are randomly reorienting between the *p*- and *h*-orientation. Therefore, the time-averaged interaction potential is a linear combination of the potentials mentioned above and also has S_6 symmetry. The energy difference between the minima on and off the C_3 symmetry axis of this time-averaged potential as a function of the probability *p* of finding a C$_{60}$ molecule in the *p*-orientation can be expressed as

$$\Delta E(p) = p\Delta E_p + (1-p)\,\Delta E_h = (54p - 6) \text{ cm}^{-1} \quad (1)$$

At temperatures below the glass-transition temperature, the C$_{60}$ molecules surrounding the CO molecule are randomly frozen in either the *p*- or the *h*-orientation in a 12.5:1 ratio. If all six of the C$_{60}$ molecules surrounding the CO molecule are *p*-oriented (63% of the sites), the symmetry of the CO potential is, to a good approximation, still S_6; however, if one (or more) of the six C$_{60}$ molecules is (are) *h*-oriented (the remaining 37% of the sites), the symmetry of the CO potential is lowered or even lost (C_1 symmetry).

Experimental Section

Sample Production. CO-intercalated C$_{60}$ samples are produced by high-pressure, high-temperature synthesis by using typically several hundred bar of CO gas at a temperature of several hundred °C for a period of a few days.[1] Two samples, denoted no. 1 and no. 2, are used in this study. Polycrystalline C$_{60}$ powder (Hoechst, Super Gold Grade, purity >99.9%) is first heated in a vacuum to 350 °C for half a day to remove residual solvent. Then, the purified C$_{60}$ powder (sample no. 1, 100 mg; sample no. 2, 500 mg) is crushed and put into a quartz container which is placed in a high-pressure vessel (Parr Instrument, *p* ≤ 580 bar and *T* ≤ 350 °C). The remaining volume of the high-pressure vessel is filled with stainless steel rods. The production of [13]CO (99 atom % [13]C)-intercalated C$_{60}$ samples is somewhat more involved than the production of samples containing CO in natural abundance as [13]CO gas is supplied in lecture bottles at low-pressure only. The 99 atom % [13]C enriched [13]CO gas (sample no. 1: 2.2 bar·0.45 L from Aldrich; sample no. 2, 11.0 bar·0.45 L from Isotec) is cryopumped into the high-pressure vessel by cooling the vessel down to liquid nitrogen temperature. Since the vapor pressure of CO at 77 K is approximately 0.7 bar, a substantial amount of the [13]CO gas can be transported into the high-pressure vessel in this way. After the high-pressure vessel is heated to a temperature of 250 °C, pressures of 75 and 400 bar [13]CO are reached during the production of samples no. 1 and no. 2, respectively. The samples are left under these conditions for a prolonged time, i.e., 3 days for sample no. 1 and 9 days for no. 2. After the high-pressure vessel is cooled to room temperature, the excess [13]CO gas is cryopumped back into the lecture bottle. The [13]CO-intercalated C$_{60}$ samples are stored in a freezer at −70 °C until they are used. For the measurements of the chemical shift anisotropy tensor of solid [13]CO a sealed quartz ampule containing approximately 25 bar of [13]CO gas is prepared.

Solid-State ^{13}C NMR Measurements. The static solid-state ^{13}C NMR measurements on [13]CO-intercalated C$_{60}$ have been performed on a home-built spectrometer[19] with an Oxford 5.17 T magnet (^{1}H, 220.0 MHz; ^{13}C, 55.31 MHz) using a home-built, variable-temperature NMR probe.[20] The NMR probe fits into an Oxford Instruments liquid helium flow cryostat. The liquid helium flow is used to cool a massive copper block which encloses the radio frequency (rf) coil and the sample. The sample is cooled by heat exchange with the cooled copper block via helium gas present in the probe housing. The temperature of the copper block can be regulated between 4 and 298 K. The temperature of the sample in the rf coil is equal to the temperature of the copper block within 1 K.[20] The electrical tuning elements for the [13]C−[1]H double-resonance tuning circuit are placed outside the cryostat. The rf-radiation is conducted to the 11-mm diameter solenoid coil (5 turns) by a beryllium−copper semirigid coaxial cable with a Teflon dielectricum and a length equal to the wavelength λ_H ($\lambda_C/4$) of the rf radiation required for protons (carbon atoms). The rf coil is formed from the inner part of the coaxial cable with the outer shield carefully removed to leave the Teflon insulation undamaged.[20] Empirically, it is found that the homogeneity of the magnetic field decreases at temperatures below 100 K, leading to an instrumental line-broadening on the order of 20 ppm at 4 K. We tentatively attribute this (reversible) broadening to magnetization of either the cryostat and/or parts of the probehead at low temperatures.

When measuring the ^{13}C NMR signal (using a single rf pulse) of the probe without a sample, a strong and relatively broad [full width at half-maximum (fwhm) of 50 ppm] background signal is observed centered at a chemical shift of approximately 110 ppm relative to TMS. This signal originates from ^{13}C atoms in the Teflon insulation of the rf coil and can be efficiently suppressed by a Hahn-echo sequence[21] with a delay of $\tau = 300$ μs. Because of the strong dipolar coupling between the ^{13}C and ^{19}F spins in the Teflon, the homogeneous ^{13}C line width exceeds 2.5 kHz, and no echo signal of Teflon can be observed for the τ used. For CO and C$_{60}$, the homogeneous line width is much smaller (≤200 Hz), and the signal can be almost fully refocused by the Hahn-echo sequence. The rf field strength has been set to 25 kHz, and the dwell-time for detection to 20 μs. A zeroth- and first-order phase correction and a linear baseline correction are applied to the spectra.

^{13}C NMR spectra under magic-angle spinning (MAS) conditions have been obtained by single rf pulse excitation on two different instruments, a AM500 spectrometer (Bruker) equipped with a solid-state accessory using a 5-mm CP-MAS probehead (Doty Scientific) and a DMX300 spectrometer (Bruker) using a 4-mm CP-MAS probehead (Bruker).

Results

Determination of the CO to C$_{60}$ Ratio. The ratios of [13]CO to C$_{60}$ in both of the CO-intercalated C$_{60}$ samples have been determined from MAS spectra at room temperature. The spectra of samples no. 1 and no. 2 have been measured in a magnetic field of 11.74 and 7.04 T, respectively. The T_1 relaxation time of [13]CO in the CO-intercalated C$_{60}$ sample is 1.7 s at room temperature and is found to be almost independent of the magnetic field strength in the range of fields used in this study. The T_1 relaxation time of C$_{60}$ is much longer and depends strongly on the magnetic field strength, i.e., about 30 s at 11.74 T and about 78 s at 7.04 T. Therefore, relaxation delays of 125 s for sample no. 1 measured at 11.74 T and of 400 s for sample no. 2 measured at 7.04 T have been used for the quantitative MAS NMR spectra shown in Figure 1. Two sharp resonances are observed at 142.6 and 183.9 ppm which can be assigned to C$_{60}$ (pure C$_{60}$, 143 ppm[5]) and CO (pure CO, 182 ppm[22]). From the integrated intensities of the NMR resonances, the ratio of CO to C$_{60}$ in the CO-intercalated C$_{60}$ samples is determined

(19) Hediger, S.; Signer, P.; Tomaselli, M.; Ernst, R. R.; Meier, B. H. *J. Magn. Reson.* **1997**, *125*, 291−301.

(20) Schaffhauser, T. B. *Ph.D. Thesis No. 7439*; ETH Zürich, 1983. Copies available upon request per e-mail: beme@nmr.phys.chem.ethz.ch.

(21) Hahn, E. L. *Phys. Rev.* **1950**, *80*, 580−594.

(22) Beeler, A. J.; Orendt, A. M.; Grant, D. M.; Cutts, P. W.; Michl, J.; Zilm, K. W.; Downing, J. W.; Facelli, J. C.; Schindler, M. S.; Kutzelnigg, W. *J. Am. Chem. Soc.* **1984**, *106*, 7672−7676.
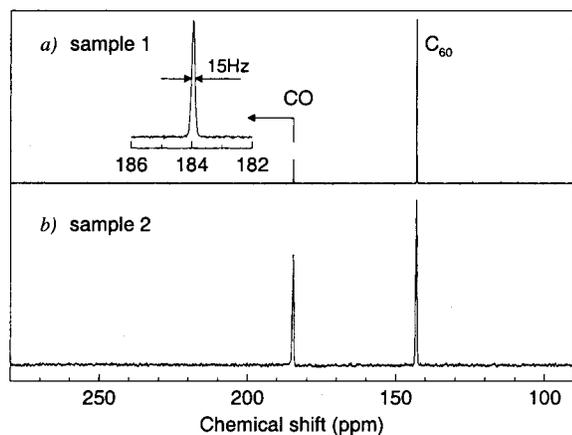
Figure 1. (a) ^{13}C NMR spectrum of ^{13}CO-intercalated C_{60} sample no. 1 measured in the AM500 spectrometer under magic-angle-spinning conditions at room temperature. This spectrum is recorded by summing 30 scans using a relaxation delay of 125 s. The inset shows an expanded view of the observed CO resonance. (b) The same for sample no. 2, but recorded on the DMX300 spectrometer by summing 16 scans with a relaxation delay of 400 s. The chemical shift in both spectra is referenced to tetramethylsilane (TMS).

(using the known ^{13}C abundance of 99% in ^{13}CO gas and of 1.1% in C_{60}) as 1:9.1(4) for sample no. 1 and as 1:2.1(1) for sample no. 2. The longer exposure time and the higher pressure of the ^{13}CO gas during the production of sample no. 2 compared to that of sample no. 1 have resulted in a significantly higher filling ratio for sample no. 2, which is, however, still a factor of 2 lower than the theoretically maximum filling ratio of 1:1. From a recent X-ray study on a CO-intercalated C_{60} sample (produced under conditions similar to those of our sample no. 2) the ratio of CO to C_{60} has been determined as 1:1.5(1).[17] The inset of Figure 1a shows the NMR resonance of CO in CO-intercalated C_{60} on an expanded scale. No evidence is found for the presence of a second CO resonance, and therefore it seems unlikely that a substantial fraction of the CO molecules is either sharing an octahedral site or is intercalated in the much smaller tetrahedral sites.

Static ^{13}C NMR Spectra of CO-Intercalated C_{60}. In Figure 2a series of static NMR spectra of sample no. 2 in the 295 to 30 K region is shown. The relaxation delay between scans has been set to 10 s, sufficiently long to have full relaxation of ^{13}CO. For C_{60}, this delay is too short and the signal becomes attenuated. The fwhm of the symmetric ^{13}CO resonance is 6.8 ppm, only a fraction of the chemical shift anisotropy (CSA) tensor of solid ^{13}CO which exceeds 350 ppm[23] (vide infra). This implies, in agreement with expectations, that the CO molecules in the CO-intercalated C_{60} sample reorient rapidly in an environment with a high symmetry (O_h) which averages the second-rank CSA tensor to its isotropic value. Upon the temperature being lowered, the line shape of the CO resonance abruptly changes, between 245 and 235 K, into a tensor pattern. Below 235 K, the anisotropy of the CO tensor increases steadily with decreasing temperature. The sign of the CSA anisotropy is inverted with respect to that of solid polycrystalline CO, and the edge singularity (the highest intensity in the powder pattern) of the CSA tensor of CO in solid C_{60} appears at the most shielded position, i.e., at low ppm values.

The observed NMR resonance of C_{60} at room temperature is also symmetric with a line width (fwhm) of 5.0 ppm. Upon temperature being lowered, the line shape of the C_{60} resonance
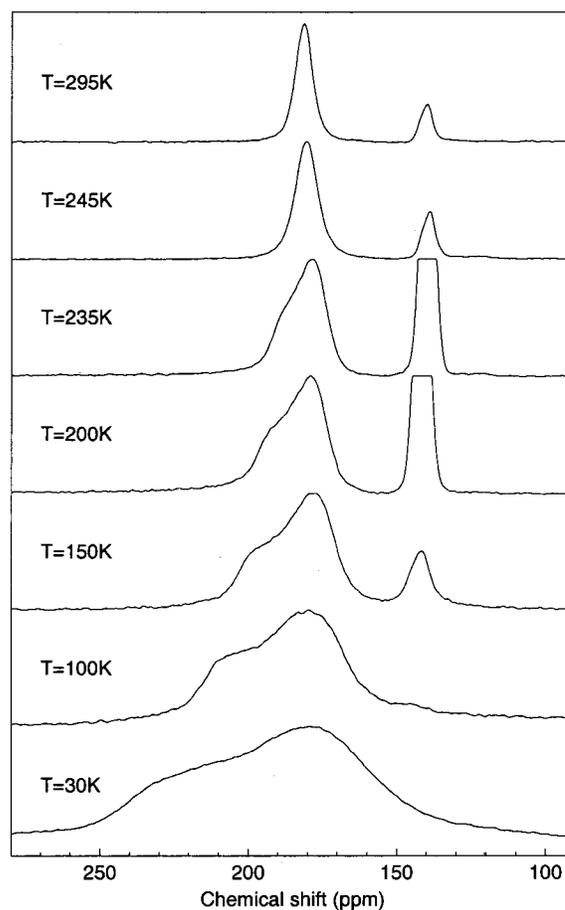
(23) Gibson, A. A. V.; Scott, T. A.; Fukushima, E. *J. Magn. Reson.* **1977**, *27*, 29−33.

Figure 2. Static ^{13}C NMR spectra of ^{13}CO-intercalated C_{60} (sample no. 2) measured as a function of temperature in a magnetic field of 5.17 T. Each spectrum consists of approximately 1000 scans which are recorded using a relaxation delay of 10 s, except for the spectra at 100 and 30 K which are measured using a delay of 30 s. Due to magnetization of the probehead at low temperatures the isotropic chemical shift values of CO and C_{60} appear to move to higher chemical shift values for 100 and 30 K.

remains symmetric down to 150 K, but its intensity changes drastically between 245 and 235 K due to changes in the relaxation behavior (shortening of T_1) in combination with the short relaxation delay used in recording the spectra. In the temperature region between 150 and 100 K, the symmetric resonance of C_{60} changes into a CSA tensor pattern which is partly overlapping with the line shape of CO.

In Figure 3 a series of static ^{13}C NMR spectra of CO-intercalated C_{60} (sample no. 2) in the 3 K to 4 K region is shown. Note the difference by a factor of in the horizontal scale between this figure and Figure 2. At these low temperatures, a summation of over eight scans is sufficient to obtain a static NMR spectrum with a good signal-to-noise ratio. The relaxation delay used in recording these spectra is set at 600 s in order to account for the increased T_1 of CO. Due to this long relaxation delay, the interfering signal of the CSA tensor of C_{60} is much stronger in these spectra, which hampers a direct analysis of the spectra. By comparing the static NMR line shape of CO-intercalated C_{60} at 4 K to the CSA tensor of pure CO and of pure C_{60} (see Figure 4a and b), it is evident that the spectrum of CO-intercalated C_{60} is the sum of both. When the temperature of the sample increases to 7 K or higher, the spectral shape of the contribution of CO to the total NMR spectrum changes rapidly, as is most clearly seen from the vanishing of the discontinuity in the NMR spectrum at approximately 320 ppm. At 30 K, the

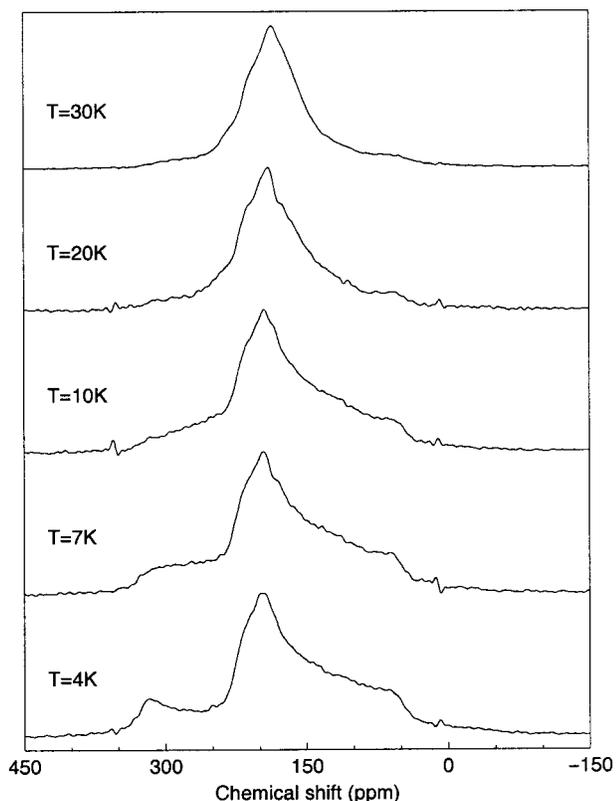**Figure 3.** Static ^{13}C NMR spectra of ^{13}CO-intercalated C_{60} (sample no. 2) measured as a function of temperature in a magnetic field of 5.17 T. A relaxation delay of 600 s and 8 scans have been used in recording these spectra. The apparent increase of the isotropic chemical shift values of CO and C_{60} with decreasing temperature is an experimental artifact.

CO line shape has merged with the powder pattern of C_{60}, and the two contributions are hard to separate visually.

Measurement of the CSA Tensors of CO and C_{60}. Although the principle values of the CSA tensors of both of the solid CO[22,23] and C_{60}[5,7] are known, we remeasured both CSA tensors in our setup. The ^{13}C NMR spectrum of solid CO at 4 K is shown in Figure 4a (solid curve). From a fit to an axially symmetric tensor, shown in Figure 4a as the dashed curve, the anisotropy of the CSA tensor of solid ^{13}CO is determined as $\delta_{\perp} - \delta_{\parallel} = 362 \pm 2$ ppm. This value is, within error, equal to the value at 4 K reported by Gibson et al.[23] Note that, in contrast to the CO tensor in Figure 2, the edge singularity is found at the least shielded position.

The CSA tensor of pure C_{60}, shown in Figure 4b (solid curve), has been measured at a temperature of 50 K. When the C_{60} sample is cooled to 4 K, a thus far unexplained broadening appeared which made it impossible to record a decent powder pattern of C_{60} at this temperature. From a fit of the powder pattern at 50 K to a second-rank tensor, shown in Figure 4b as the dashed curve, the parameters describing the shape of the CSA tensor of C_{60} are obtained as $\delta_{33} - \delta_{iso} = -111 \pm 1$ ppm and $\delta_{22} - \delta_{11} = -32 \pm 1$ ppm. These values correspond within 2 ppm to those reported previously.[5,7]

Broadening of the CO Resonance. In Figure 5a and b a comparison is made between the static NMR line shapes of CO at room temperature measured in two different magnetic fields. The width of the CO resonance line in the low magnetic field is partly caused by the probe ($\sim$125 Hz) but is still substantially smaller than the width of the resonance line in the high magnetic field. This indicates that the dominant contribution to the CO
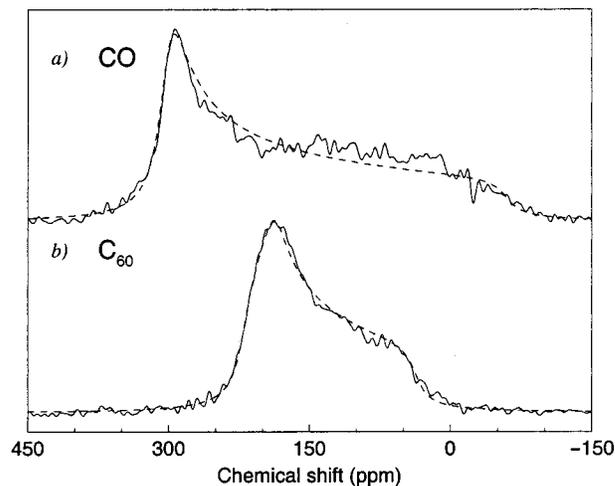

Figure 4. (a) CSA tensor of solid ^{13}CO (solid curve) at a temperature of 4 K measured in a magnetic field of 5.17 T by summing 64 scans and using a relaxation delay of 30 s. From a fit to an axially symmetric tensor (dashed curve) the anisotropy of the CSA tensor of ^{13}CO is determined as $\delta_{\perp} - \delta_{\parallel} = 362 \pm 2$ ppm. (b) The CSA tensor of C_{60} (solid curve) at a temperature of 50 K recorded using 0.5 g of polycrystalline C_{60} powder (Hoechst, Super Gold Grade, purity >99.9%) which has been heated in a vacuum to remove residual solvent. The C_{60} spectrum is measured in a magnetic field of 5.17 T by summing 200 scans using a relaxation delay of 300 s. From a fit of the experimental curve to a second-rank tensor (dashed curve) the parameters of the CSA tensor of C_{60} are obtained as $\delta_{33} - \delta_{iso} = -111 \pm 1$ ppm and $\delta_{22} - \delta_{11} = -32 \pm 1$ ppm. Both CSA tensors have been shifted so that their isotropic shift values match the values deduced from Figure 1.
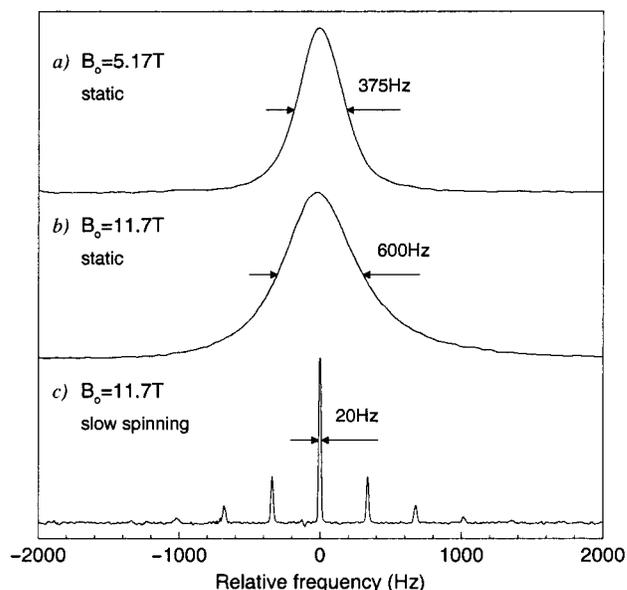

Figure 5. (a) Static ^{13}C NMR line shape of CO in CO-intercalated C_{60} (sample no. 2) at room temperature measured in a 5.17 T magnet (10 s relaxation delay, 1500 scans). (b) The static ^{13}C NMR line shape of CO in CO-intercalated C_{60} (sample no. 1) at room temperature measured in the AM500 spectrometer (11.74 T). (6 s relaxation delay, 12,000 scans). (c) The slow MAS ^{13}C NMR spectrum of CO in CO-intercalated C_{60} (sample no. 1) at room temperature in the AM500 spectrometer using a spinning speed of 350 Hz. (6 s relaxation delay, 80 scans). The horizontal axis indicates the frequency relative to the isotropic resonance frequency of CO in CO-intercalated C_{60}.

line broadening scales, in this magnetic field region, with the strength of the magnetic field. Since the magnetic dipolar coupling is independent of the magnetic field strength, it is

concluded that the $^{13}C-^{13}C$ dipolar coupling cannot be the dominant broadening mechanism of the CO line. A crude estimate of the broadening of the line of CO caused by dipolar coupling with the six surrounding C_{60} molecules yields a contribution to the line width of 200 Hz, which therefore may still explain a substantial part of the observed line width. In Figure 5c a spinning sideband spectrum of CO-intercalated C_{60} recorded at room temperature using slow magic-angle spinning (350 Hz) is shown. The observation of a set of narrow sidebands from the CO line shape finds evidence that the line broadening originates from an effect that gives rise to one (or a distribution of) second-rank tensor(s). By fitting the measured slow-spinning spectrum to the sideband intensities of a single tensor using the tables of Herzfeld–Berger[24] a poor fit is obtained. By using a sum of axial tensors with a Gaussian distribution of anisotropies (fwhm of 12 ppm), however, the observed sideband pattern can be adequately reproduced. These observations are in agreement with a CO line shape which mainly originates from isotropic bulk magnetic susceptibility broadening.[25]

Modeling of the ^{13}C NMR Spectra. The isotropic chemical shift of ^{13}CO is assumed to be identical for the eight possible orientations of CO in the octahedral site. Although this is enforced by symmetry in the fcc phase, it is expected to be a good approximation for the low-temperature phase, and experimentally no evidence for the contrary is found. If the motion is frozen, the MAS spectrum consists of one line, whereas the single crystal spectrum (in a general orientation) consists of four lines (the two possible orientations along the same cube diagonal yield the same chemical shift) due to the spatial asymmetry of the chemical shift tensor. The powder spectrum, on the other hand, consists again of a single chemical shift tensor pattern. When the jump rate is much higher than the width of the CSA tensors (fast-exchange limit), the MAS spectrum still consists of one line, while the single crystal spectrum now also yields a single line at the mean frequency of the four lines in the absence of exchange, and its position will in general be orientation dependent. For a powder sample, a partially averaged tensor results. For the special case where all eight minima are equally occupied, an isotropic line appears. For fast-exchange between the six equivalent minima of the S_6 potential only, the averaged tensor will be scaled by a factor of $-1/3$ with respect to the CO tensor. For fast-exchange between the two equivalent minima of the S_6 potential only, no scaling of the tensor will be observed since the tensor is invariant under a 180° rotation. In the general case it follows, therefore, that the averaged tensor will have a negative scaling factor, i.e., the sign of the asymmetry will be inverted, with respect to that of solid CO when the six equivalent minima of the S_6 potential are lower in energy than the remaining two (local) minima.

The Chemical-Exchange Model. Using the information on the structure of CO-intercalated C_{60} as given in the Introduction as input, we have constructed a model to calculate the static NMR spectra of CO-intercalated C_{60} as a function of temperature. In this model, based on classical chemical-exchange,[13,26] the rovibrational motion of CO in the C_{60} potential is approximated by jumping between eight discrete orientations. In the schematic drawing shown in Figure 6a each of the eight discrete minima is represented by a black dot on the corner of a cube. Each of these minima corresponds to an orientation of the CO molecule along a specific cube diagonal, with the oxygen
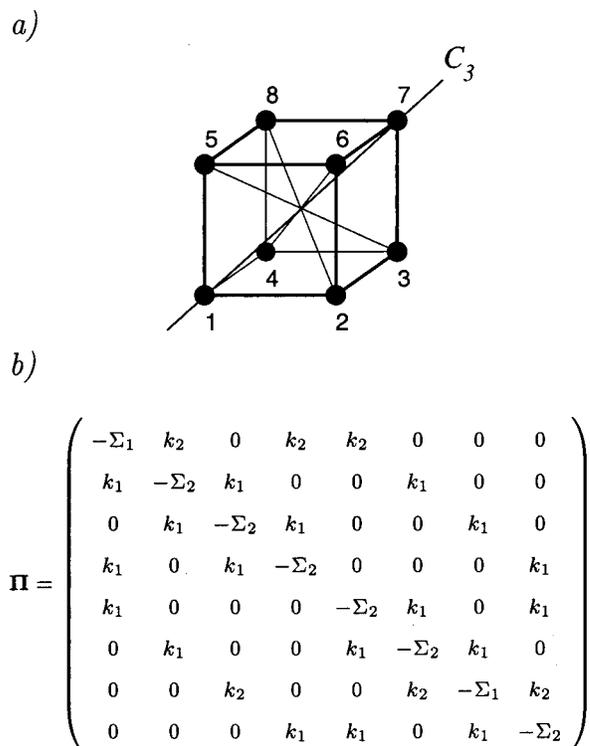
(24) Herzfeld, J.; Berger, A. E. *J. Chem. Phys.* **1980**, *73*, 6021–6030.
(25) VanderHart, D. L.; Earl, W. L.; Garroway, A. N. *J. Magn. Reson.* **1981**, *44*, 361–401.
(26) Gutowsky, H. S.; McCall, D. W.; Slichter, C. P. *J. Chem. Phys.* **1953**, *21*, 279–292.

a)

b)

$$\Pi = \begin{pmatrix} -\Sigma_1 & k_2 & 0 & k_2 & k_2 & 0 & 0 & 0 \\ k_1 & -\Sigma_2 & k_1 & 0 & 0 & k_1 & 0 & 0 \\ 0 & k_1 & -\Sigma_2 & k_1 & 0 & 0 & k_1 & 0 \\ k_1 & 0 & k_1 & -\Sigma_2 & 0 & 0 & 0 & k_1 \\ k_1 & 0 & 0 & 0 & -\Sigma_2 & k_1 & 0 & k_1 \\ 0 & k_1 & 0 & 0 & k_1 & -\Sigma_2 & k_1 & 0 \\ 0 & 0 & k_2 & 0 & 0 & k_2 & -\Sigma_1 & k_2 \\ 0 & 0 & 0 & k_1 & k_1 & 0 & k_1 & -\Sigma_2 \end{pmatrix}$$

Figure 6. (a) Schematic view of the directions along which the internuclear axis of the CO molecule is oriented in the eight discrete minima which are used in the chemical-exchange model for the NMR line shape of CO in the C_{60} cavity. (b) The chemical-exchange matrix Π which describes the reorientation of the CO molecule between the eight discrete minima. k_1 is the rate constant for jumping to one of the six equivalent minima 2–6,8 and k_2 is the rate constant for jumping to the two equivalent minima 1 and 7. The elements on the diagonal of Π are $\Sigma_1 = 3k_1$ and $\Sigma_2 = 2k_1 + k_2$.

atom pointing in the direction of the marked corner. The eight orientational minima are characterized by the energy of the CO molecule in that minimum. In a potential with S_6 symmetry the two minima on the C_3 axis (1 and 7) have the same energy, and the other six minima off the C_3 axis are also equivalent. The energy difference between the two equivalent minima (1 and 7) and the other six equivalent minima is denoted ΔE. When this energy difference ΔE is set to zero, all of the eight minima are equivalent, and a potential with O_h symmetry is obtained. The jumping of a CO molecule between the different minima in this potential is described by an exchange matrix Π containing the rate constants Π_{ij} for a CO molecule jumping from minimum i to minimum j. The diagonal element Π_{ii} of the exchange matrix is equal to the total rate constant for jumping out of the corresponding minimum i (details in ref 27).[27] In setting up the exchange matrix of Figure 6b, it is assumed that a CO molecule can only jump to a neighboring minimum, i.e., it can only jump via the edges of the cube shown in Figure 6a. In this matrix, k_1 is the rate constant for jumping to one of the six equivalent minima, and k_2 is the rate constant for jumping to one of the two equivalent minima. The ratio between k_1 and k_2 is related to the energy difference between the minima: $k_2 = k_1 \exp(-\Delta E/R\,T)$ (R: the Boltzmann constant, T: the temperature). The static NMR spectrum of a CO molecule in this eight minima model can be calculated for a single crystallite by using the McConnell modification of the Bloch equations for classical chemical-exchange[13]

(27) Ernst R. R.; Bodenhausen, G.; Wokaun, A. *Principles of nuclear magnetic resonance in one and two dimensions*; Oxford Science Publications: Oxford, 1987; pp 57–63.

$$\partial/\partial t \vec{G}(\alpha,\beta,t) = (i\boldsymbol{\Omega}(\alpha,\beta) - \boldsymbol{\Lambda} + \boldsymbol{\Pi})\, \vec{G}(\alpha,\beta,t) \equiv$$
$$\mathbf{S}(\alpha,\beta)\, \vec{G}(\alpha,\beta,t) \quad (2)$$

In this equation, $\vec{G}(\alpha,\beta,t)$ is a vector containing the complex magnetizations of each of the eight minima ($G^{(j)} = M_x^{(j)} + iM_y^{(j)}$), $\boldsymbol{\Pi}$ is the exchange matrix described above, $\boldsymbol{\Lambda}$ is a diagonal matrix containing the transverse relaxation rates ($1/T_2$), and $\boldsymbol{\Omega}(\alpha,\beta)$ is a diagonal matrix containing the angular resonance frequencies of ^{13}CO in each of the eight minima. The NMR signal as a function of time (FID) is just the sum over the eight components of the magnetization vector $\vec{G}(\alpha,\beta,t)$, i.e., $\vec{e}\cdot\vec{G}(\alpha,\beta,t)$ with $\vec{e} = (1, 1, ..., 1)$. The Euler angles (α,β) describe the relative orientation of the molecule-fixed coordinate system (the cube of Figure 6a) and the magnetic field vector. The transverse relaxation rates of the CO molecule in the eight different minima, contained in the $\boldsymbol{\Lambda}$ matrix, are all assumed to be equal and independent of (α,β). An expression for the NMR signal as a function of time $\vec{e}\cdot\vec{G}(\alpha,\beta,t)$ and its Fourier transform $\vec{e}\cdot\vec{g}(\alpha,\beta,\omega)$ in terms of the complex eigenvalues and eigenvectors of $\mathbf{S}(\alpha,\beta)$ and the initial magnetization vector $\vec{G}(\alpha,\beta,t_0)$ can be obtained.[28]

After applying the Hahn-echo sequence on the complex magnetization vector, the NMR spectrum of a CO molecule jumping in the minima cube at a specific orientation (α,β) is now constructed by using the expression for $\vec{e}\cdot\vec{g}(\alpha,\beta,\omega)$ and the numerically obtained eigenvalues and eigenvectors of $\mathbf{S}(\alpha,\beta)$. The powder line shape is obtained by adding the contributions of the single crystallites, using the method of Cheng et al.[29] The spectrum of a C$_{60}$ molecule, which at low temperature is overlapping the spectrum of CO, is approximated in the model by a combination of an isotropic line (high-temperature spectra) and a CSA tensor (low-temperature spectra) calculated using the constants obtained from the fit shown in Figure 4b. The total calculated static NMR spectrum of CO-intercalated C$_{60}$, which is the sum of the CO and the C$_{60}$ contribution, is convoluted with a single Gaussian or a single Lorentzian line shape function. The transverse relaxation broadening $\Delta\nu_{T_2}$ of CO in the exchange model is used to account for the difference between the line broadening of CO and C$_{60}$.

Results of the Model and Discussion

The Model under Fast-Exchange. All measured static NMR spectra of both CO-intercalated C$_{60}$ samples have been fitted to the chemical-exchange model described above. In Figure 7 a selection of spectra from Figure 2 (solid curves) are shown together with their best fit (dashed curves). From both the measured and the fitted spectra shown in this figure the fitted C$_{60}$ contribution has been subtracted to get a clear picture of the shape of the CSA tensor of CO as a function of the temperature. The sharp C$_{60}$ NMR line is well-reproduced by a pure Gaussian line shape in the 298 to 150 K temperature region and only a wiggle around 140 ppm remains after subtraction of this line shape from the measured spectra. The rate constant k_1 is not a stable fit parameter in the 298 to 100 K temperature region because these spectra are in the fast-exchange limit and the exchange rate is highly correlated with $\Delta\nu_{T_2}$ describing the additional broadening of the CO line shape. Therefore, k_1 is fixed at a high value (essentially infinite) during the fitting. In Table 1 an overview of the nontrivial parameters belonging to the fitted spectra in the fast-exchange limit shown in Figure 7 is given.
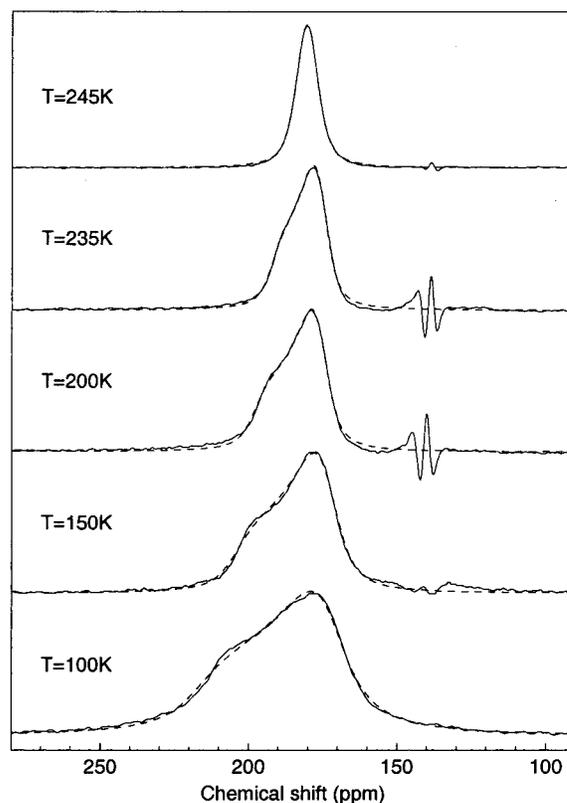
(28) Spiess, H. W. *NMR: Basic Principles and Progress*; Springer-Verlag: Berlin, 1978; Vol. 15, pp 93−98.
(29) Cheng, V. B.; Suzukawa, H. H.; Wolfsberg, M. *J. Chem. Phys.* **1973**, *59*, 3992−3999.
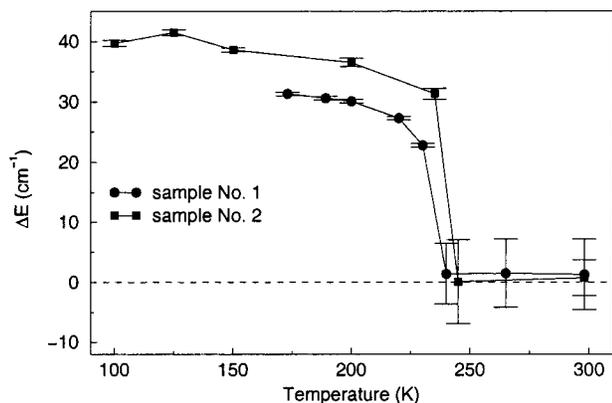

Figure 7. Comparison of the static NMR spectra of sample no. 2 measured in 5.17 T magnet (solid curves) and the calculated spectra fitted with the chemical-exchange model described in the text (dashed curves) as a function of temperature in the 245 K to 100 K region. From both the measured and the calculated spectra the fitted C$_{60}$ line shape has been subtracted.

Table 1. Overview of the Nontrivial Parameters (Apart from Scaling and Shifting Parameters) Belonging to the Fitted Spectra Shown in Figure 7[a]

T (K)	k_1[b] (GHz)	ΔE[c] (cm^{-1})	$\Delta\nu_{T_2}$[d] (ppm)	R_{iso}[e]	R_{tens}[f]	$\Delta\nu_G$[g] (ppm)
298	1.0	1(3)	3.1(2)	0.189(4)	0.0	5.0(1)
245	1.0	0(7)	5.2(2)	0.186(4)	0.0	5.4(1)
235	1.0	31.3(9)	4.7(4)	0.99(2)	0.0	5.0(1)
200	1.0	36.5(7)	5.7(3)	0.78(1)	0.0	5.5(1)
150	1.0	38.6(3)	7.7(2)	0.140(3)	0.0	8.7(2)
125	1.0	41.5(5)	14.6(7)	0.050(3)	0.57(2)	8.7(4)
100	1.0	39.7(5)	17.9(5)	0.0007(2)	0.81(2)	7.0(6)

[a] The value between parentheses is the uncertainty in the last digit. When this value is omitted, the corresponding parameter has been fixed during the fitting. [b] The rate constant for jumping to one of the six equivalent minima ($k_2 = k_1 \exp(-\Delta E/RT)$). [c] The energy difference between the two equivalent minima and the six equivalent minima. [d] The full width at half-maximum (fwhm) of the additional Lorentzian line broadening of the CO line shape. [e] The area ratio of the C$_{60}$ isotropic line to the CO line shape. [f] The area ratio of the C$_{60}$ tensor to the CO line shape. [g] The fwhm of the overall Gaussian broadening of the spectrum.

In Figure 8 the energy difference between the two equivalent minima on the C_3 axis and the six equivalent minima off the C_3 axis (ΔE) as obtained from the fitting of the measured NMR spectra of samples no. 1 and no. 2 to the exchange model is plotted as a function of temperature. In the range between room temperature and 245 K, the obtained values for ΔE indicate no significant deviation from an octahedral symmetry of the CO potential ($\Delta E = 0 \leftrightarrow O_h$). The abrupt change of the line shape of CO between 245 and 235 K corresponds in the chemical-exchange model to an abrupt change of ΔE from around zero

Figure 8. Plot of ΔE, i.e., the energy difference between the two equivalent minima on the C_3 axis and the six equivalent minima off the C_3 axis, as a function of temperature obtained from the fitting of the measured static NMR spectra of sample no. 1 (circles) and sample no. 2 (squares) to the chemical-exchange model. The static NMR spectra of CO-intercalated C_{60} sample no. 1 as a function of temperature have been measured in the AM500 spectrometer and have partly been shown elsewhere.[1]

to a distinctly nonzero value, in agreement with the symmetry lowering of the potential from O_h to S_6 in crossing the orientational ordering transition temperature. The inverted sign of the anisotropy of the dynamical CO tensor (compare Figures 2 and 4a) unequivocally points to a positive value of ΔE, implying that the CO molecules are preferentially oriented away from the C_3 symmetry axis of the site.

It is evident from Figure 8 that the value of ΔE below the phase-transition temperature is dependent on the sample, i.e., on the ratio of CO to C_{60}. The value of ΔE also depends on the temperature, and ΔE gradually increases with decreasing temperature. Using eq 1 an increase of the fraction of p-oriented C_{60} molecules is expected to lead to an increase of the observed value of ΔE. The observed trend toward higher values of ΔE with decreasing temperature is therefore in agreement with the known increase in the fraction of p-oriented C_{60} molecules when the temperature is lowered.[15] The increase of the observed ΔE values in going from the poorly loaded sample no. 1 (11% occupancy of the octahedral sites) to the better loaded sample no. 2 (48% occupancy of the octahedral sites) is consistent with the higher probability p for better loaded samples.[18] At a temperature of 150 K the probability to find p-oriented C_{60} molecules in pristine C_{60} has been determined using neutron powder diffraction as $p = 0.701$,[30] whereas for a CO-intercalated C_{60} sample similar to our sample no. 2 this has been determined using X-ray powder diffraction as $p = 0.814$.[18] Using these values, the calculated energy differences at 150 K are $\Delta E(0.701) = 32$ cm^{-1} and $\Delta E(0.814) = 38$ cm^{-1} which are, probably fortuitously, in almost perfect agreement with the experimental values for ΔE of sample no. 1 (close to pristine C_{60}) and sample no. 2.

From Fast to Slow Exchange. At temperatures below the glass-transition temperature, the chemical-exchange model for the NMR line shape of CO that we have used so far is, strictly speaking, no longer applicable because of the presence of the several differently distorted octahedral sites in the C_{60} lattice. As the chemical-exchange model is still valid for the majority of the CO molecules (63% in sample no. 2), the measured NMR spectra of CO-intercalated C_{60} between 30 and 4 K have been fitted with the chemical-exchange model anyway. In Figure 9

(30) David, W. I. F.; Ibberson, R. M.; Matsuo, T. *Proc. R. Soc. London Ser.* **1993**, *442*, 129−146.
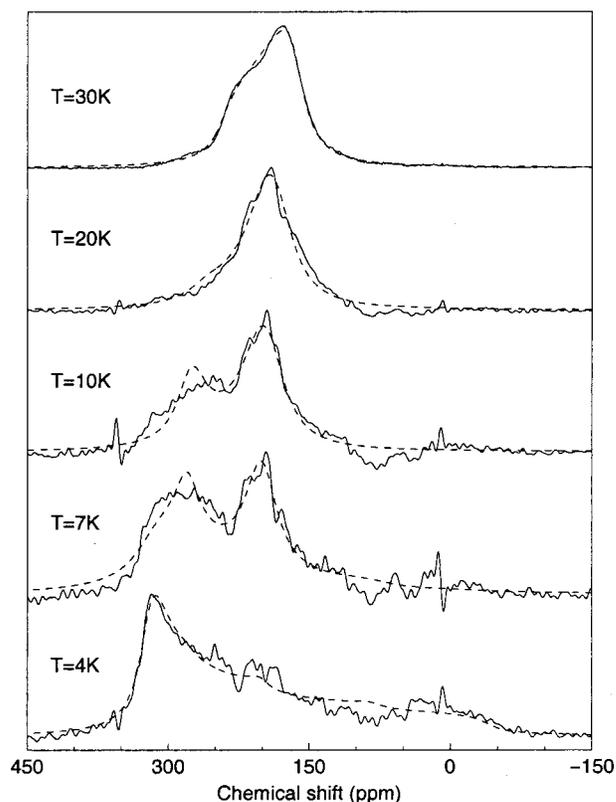

Figure 9. Comparison of the static NMR spectra of sample no. 2 measured in 5.17 T magnet (solid curves) and the calculated spectra fitted with the chemical-exchange model described in the text (dashed curves) as a function of temperature in the 30 to 4 K region. From both the measured and the calculated spectra the fitted C_{60} line shape has been subtracted.

Table 2. Overview of the Nontrivial Parameters (Apart from Scaling and Shifting Parameters) Belonging to the Fitted Spectra Shown in Figure 9[a]

T (K)	$k_1{}^b$ (kHz)	ΔE^c (cm^{-1})	$\Delta \nu_{T_2}{}^c$ (ppm)	$R_{tens}{}^c$	$\Delta \nu_L{}^d$ (ppm)
30	361(40)	25.3(3)	3.1	0.10(1)	21.2(8)
20	39(2)	25.3	3.1	0.74(1)	25.6(6)
10	20(2)	25.3	3.1	2.76(4)	24.3(4)
7	5.1(2)	25.3	3.1	2.72(3)	22.4(3)
4	1.5(1)	25.3	3.1	2.52(3)	12.3(3)

[a] The value between parentheses is the uncertainty in the last digit. When this value is omitted, the corresponding parameter has been fixed during the fitting. [b] The meaning of the parameter is described in a footnote of Table 1. [c] The fwhm of the overall Lorentzian broadening of the spectrum.

the measured static NMR spectra of CO-intercalated C_{60} (sample no. 2) (solid curves) in the 30 to 4 K temperature region are shown together with their best fit (dashed curves). From both the measured and the fitted spectra shown in this figure, the fitted CSA tensor of C_{60} has been subtracted, making the peculiar behavior of the measured CO line shape in this temperature region directly visible. In Table 2 an overview of the nontrivial parameters belonging to the fitted calculated spectra shown in Figure 9 is given.

The NMR spectra of CO in this temperature region reflect the transition from the situation where the CO molecules are rapidly jumping between the different minima to the situation where the CO molecules are localized in one minimum on the NMR time scale. This time scale is determined by the anisotropy of the CSA tensor of CO in the magnetic field, and in a magnetic field of 5.17 T it is on the order of 50 μs. In this transition region the experimental line shapes of CO can still be fitted

rather well with the chemical-exchange model. The presence of the different sites and the high correlation of some parameters (e.g., the rate constant k_1 and the line width $\Delta\nu_L$) make it difficult, however, to interpret the obtained values for the fit parameters. At 4 K, the CO molecules are in the slow-exchange limit, and therefore the line shape of CO at this temperature resembles the CSA tensor of solid CO.

From the fit of the NMR line shape of CO at 4 K the rate constant for jumping from one minimum to another is determined to be lower than 1.5 kHz. This rules out the presence of quantum mechanical coherent tunneling of the CO molecules between the six equivalent minima of the octahedral sites with S_6 symmetry as is predicted from quantum mechanical calculations on CO-intercalated C$_{60}$.[1] The absence of this coherent tunneling motion can be rationalized by disturbances in the S_6 symmetry of the potential due to zero-point librational motion of the C$_{60}$ molecules in the lattice. From neutron-scattering studies on pristine C$_{60}$, these zero-point librations are expected to have an amplitude of approximately two degrees.[16] Preliminary energy level calculations indicate that this is indeed sufficient to quench the tunnel motion.

Conclusions

^{13}CO gas can be intercalated in polycrystalline C$_{60}$ in an almost 1:2 ratio as determined from MAS ^{13}C NMR measurements. Solid-state ^{13}C NMR spectra of ^{13}CO-intercalated C$_{60}$ have been measured from room temperature down to liquid helium temperature. A chemical-exchange model is constructed to describe the jump reorientations of a CO molecule in an octahedral site of the C$_{60}$ lattice. In the region between room temperature and 100 K, the CO molecules jump rapidly on the NMR time scale between different orientations in the octahedral sites of the C$_{60}$ lattice (fast-exchange). The observed inverted sign of the anisotropy of the CSA tensor of CO in solid C$_{60}$ in this temperature region compared to that of solid CO implies a preference of the CO molecule to be aligned away from the C_3 symmetry axis of the octahedral site. When cooling from 30 to 4 K, a transition from the fast-exchange limit to the slow-exchange limit is directly discernible in the static ^{13}C NMR spectra of CO. From the rate constant for jumping between different minima at 4 K, it is concluded that the coherent tunneling motion of CO in the symmetric site as predicted by quantum mechanical calculations is absent.